Probing R-parity violation in the production of $t\bar{c}$ $(c\bar{t})$ at lepton colliders[★]

Z.-H. Yu[1,3], H. Pietschmann[1], W.-G. Ma[2,3], L. Han[3], Y. Jiang[3]

[1] Institut für Theoretische Physik, Universität Wien, 1090 Vienna, Austria
[2] CCAST (World Laboratory), P.O. Box 8730, Beijing 100080, P.R. China
[3] Department of Modern Physics, University of Science and Technology of China (USTC), Hefei, Anhui 230027, P.R. China

Abstract. We studied the process $e^+e^- \to t\bar{c} + c\bar{t}$ in a R_p-violating supersymmetric model with effects from both B- and L-violating interactions. The calculation shows that it is possible to either detect the R_p-violating signal at the Next Linear Collider or get more stringent constraints on the heavy-flavor R_p couplings. A comparison with results from $\gamma\gamma \to t\bar{c} + c\bar{t}$ may allow one to distinguish between B- and L-violating interactions. For very clean background conditions and R_p-violating parameters close to the present limits, the future detection of B-violating interactions should be possible. The process of $\mu^+\mu^- \to t\bar{c} + c\bar{t}$ is also considered.

1 Introduction

In the minimal supersymmetric standard model (MSSM) [1], R-parity symmetry (R_p) is imposed on the superfield Lagrangian to guarantee the B- and L-conservation automatically. This symmetry is defined by

$$R_p = (-1)^{3B+L+2S}, \qquad (1.1)$$

where S is the spin of the particle. The discrete symmetry was introduced [2] to avoid catastrophic proton decays from R_p-violating interactions. In the models of R-parity conservation, superparticles can be only pair produced and the lightest superparticle (LSP) will be stable. Thus the LSP is a candidate for cold dark matter in the universe.

However, in order to avoid proton decay we just need either B-conservation or L-conservation [3]. Moreover, models of R_p-violation provide for neutrino masses and mixing. In those models neutrinos may get tree-level mass contributions via mixing with gauginos and higgsinos, and of course also from one-loop corrections. Unlike the general see-saw mechanism, which involves a high energy scale (about $10^{12} \sim 10^{16}$ GeV), we can explain neutrino masses with weak-scale physics. With first signals for neutrino oscillations from atmospheric neutrinos observed in Super-Kamiokande [4], R_p is getting more and more interesting.

Possible signals of R-parity violation in collider experiments have also been discussed. In the HERA e^+p deep

inelastic scattering (DIS) [5], an anomaly has been observed. It was found that the rate of neutral current (NC) events is higher than that predicted by the standard model when Q^2 is larger than $15,000$ GeV^2 (the possibility of a statistical fluctuation is about 10^{-3}). For charge current (CC) events a difference between observation and prediction of SM also exists, although not as large as for NC events. The anomaly can be explained beautifully by a R_p supersymmetric mechanism, providing a possible hint for R-parity violation.

Because R_p models open many channels forbidden or highly suppressed in R_p-conserving models, we can get many constraints from low-energy phenomenology [6]. Results are collected in [7].

Let us now consider lepton colliders. Possible ways to find a signal of R_p are as follows.
(1) Single production of sparticles and LSP decay (direct signal).
(2) Fermion pair productions are different in R_p models and in R_p-conservation models (indirect signal).
(3) Flavor changing neutral current (FCNC) and CP-violation (indirect signal).

In this paper we will concentrate on the third way. The process $l^+l^- \to f_J f_{J'}$ (J and J' are different flavors) is calculated from the L-violating terms of R_p models [8].

Although many constraints from low-energy phenomenology were already given, R_p parameters involving heavy flavors are not strongly limited. With the assumption of family symmetry [9], we can get $\lambda_{ijk} \sim Y_{ijk}$ (where λ_{ijk} are defined in (2.1) and Y_{ijk} are Yukawa couplings). So it is still possible to detect them on future colliders in the high-energy region.

In this paper we will use $t\bar{c}$ and $c\bar{t}$ production to probe $\not{R}_p$ signals on the Next Linear Collider (NLC), the First Muon Collider (FMC) [10] and possibly also at LEP2. Compared with LEP2, NLC will have much higher luminosity and energy, providing a powerful probe. This is even more true should the FMC go into operation.

Although many processes with L-violation on lepton colliders have been calculated, B-violation effects are rarely considered. Up to now B-violation parameters involving heavy flavors are still constrained weakly. For example λ''_{2ij} and λ''_{3ij} get their strongest constraints from the width ratio of Z to leptons and hadrons, still being of order one ($O(1)$). Hence future colliders can either detect them (if they are close to the present upper limits) or strongly improve the limits.

Let us consider the possible competing processes from other sources which might be confused with $\not{R}_p$-violation:
(1) Standard model. The production of $t\bar{c}$ ($c\bar{t}$) from SM is suppressed by the GIM mechanism. The process of $e^+e^- \to t\bar{c}$ ($c\bar{t}$) was considered by Huang et al. [11]. They pointed out that the cross section of the process is about 10^{-9} fb for a c.m. energy of about 200–500 GeV, thus being a negligible background for $\not{R}_p$ effects.
(2) Two-Higgs-doublet model (THDM). In the so-called Model III of [12], which gives the strongest effects of FCNC, the process e^+e^+ $(\mu^+\mu^-) \to t\bar{c}$ was considered by Atwood et al. [12], and $\gamma\gamma \to t\bar{c}$ ($c\bar{t}$) by Jiang et al. [12]. The results show that there would be 0.1 events for $e^+e^- \to t\bar{c}$ ($c\bar{t}$) and several events for $\gamma\gamma \to t\bar{c}$ ($c\bar{t}$) for a luminosity of about 50 fb^{-1}. But the effects should be much smaller, assuming the masses of the higgses to be far from the c.m. energy of the colliders. So it will be easy to distinguish them from the effects of $\not{R}_p$-violation.
(3) MSSM with R_p-conservation. Squark mixing can generate FCNC in this model. But under the alignment assumption of Dimopoulos [13], it should be very small: mixing between up-type squarks can be as small as 10^{-3} to 10^{-5} times the KM matrix elements.

In left–right symmetric models there is also a contribution to FCNC from Z' decay. Because the mass of Z' is very large, we can omit it in our calculations, where the c.m. energy is less than 500 GeV.

After these general remarks concerning the process $l^+l^- \to t\bar{c} + c\bar{t}$, we define the supersymmetric $\not{R}_p$ interaction in Sect. 2. In Sect. 3 we give the analytical calculations of $e^+e^- \to t\bar{c} + c\bar{t}$. In Sect. 4 the numerical results of the processes $e^+e^- \to t\bar{c} + c\bar{t}$ and $\mu^+\mu^- \to t\bar{c} + c\bar{t}$ are presented. The conclusions are given in Sect. 5 and some details of the expressions are listed in the Appendix.

2 R-parity violation ($\not{R}_p$) in MSSM

All renormalizable supersymmetric $\not{R}_p$ interactions can be introduced in the superpotential [6],

$$W_{\not{R}_p} = \frac{1}{2}\lambda_{[ij]k}L_i.L_j\bar{E}_k + \lambda'_{ijk}L_i.Q_j\bar{D}_k$$
$$+ \frac{1}{2}\lambda''_{i[jk]}\bar{U}_i\bar{D}_j\bar{D}_k + \epsilon_i L_i H_u, \qquad (2.1)$$

where L_i, Q_i and H_u are SU(2) doublets containing lepton, quark and Higgs superfields, respectively, $\bar{E}_j$ ($\bar{D}_j$, $\bar{U}_j$) are the singlets of the lepton (down-quark and up-quark), and i, j are generation indices; square brackets on them denote antisymmetry in the bracketed indices.

We ignored the last term in (2.1) because its effects are rather small in our process [7,14]. So we have nine λ-type, 27 λ'-type and nine λ''-type independent parameters left. The Lagrangian density of $\not{R}_p$ (to lowest order) is given by

$$L_{\not{R}_p} = L^\lambda_{\not{R}_p} + L^{\lambda'}_{\not{R}_p} + L^{\lambda''}_{\not{R}_p}, \qquad (2.2)$$

$$L^\lambda_{\not{R}_p} = \frac{1}{2}\lambda_{[ij]k}[\tilde{\nu}_{iL}\bar{e}_{kR}e_{jL} + \tilde{e}_{jL}\bar{e}_{kR}\nu_{iL} + \tilde{e}^*_{kR}\bar{\nu}^C_{iL}e_{jL}$$
$$- \tilde{\nu}_{jL}\bar{e}_{kR}e_{iL} - \tilde{e}_{iL}\bar{e}_{kR}\nu_{jL} - \tilde{e}^*_{kR}\bar{\nu}^C_{jL}e_{iL}] + \text{h.c.},$$

$$L^{\lambda'}_{\not{R}_p} = \lambda'_{ijk}[\tilde{\nu}_{iL}\bar{d}_{kR}d_{jL} + \tilde{d}_{jL}\bar{d}^C_{kL}\nu_{iL} + \tilde{d}^*_{kR}\bar{\nu}^C_{iL}d_{jL}$$
$$- \tilde{e}_{iL}\bar{d}_{kR}u_{jL} - \tilde{u}_{jL}\bar{d}_{kR}e_{jL} - \tilde{d}^*_{kR}\bar{e}^C_{iL}u_{jL}] + \text{h.c.},$$

$$L^{\lambda''}_{\not{R}_p} = \lambda''_{i[jk]}\epsilon_{\alpha\beta\gamma}[\tilde{u}^*_{iR\alpha}\bar{d}_{kR\beta}d^C_{jR\gamma} + \tilde{d}^*_{jR\beta}\bar{u}_{iR\alpha}d^C_{kR\gamma}$$
$$+ \tilde{d}^*_{kR\gamma}\bar{u}_{iR\alpha}d^C_{jR\beta}] + \text{h.c.} \qquad (2.3)$$

From the interactions above, we find that only $L^{\lambda'}_{\not{R}_p}$ contributes to $l^+l^- \to t\bar{c}+c\bar{t}$ at tree level. So the contribution from $L^\lambda_{\not{R}_p}$ can be neglected.

The proton lifetime limit supresses the possibilities of both B-violation and L-violation and leads to the constraints [7]

$$|(\lambda \text{ or } \lambda')\lambda''| < 10^{-10}\left(\frac{\tilde{m}}{100\,\text{GeV}}\right)^2. \qquad (2.4)$$

The contributions from $L^{\lambda''}_{\not{R}_p}$ are rather weak, but they can be separated from those of $L^{\lambda'}_{\not{R}_p}$. Therefore, $L^{\lambda''}_{\not{R}_p}$ effects will be considered also.

In the past years, many limits on the parameters λ, λ' and λ'' were given from low-energy experiments. The upper limits were calculated with the assumption that only one coupling parameter is non-zero [15]. On that basis, the parameters λ, λ' and λ'' are typically less than 10^{-1}–10^{-2} $(\tilde{m}/100\,\text{GeV})^2$ [7]. Although some authors argue that the limits can be relaxed [16] if the so-called single coupling hypothesis is dropped, we shall use these upper bounds in our paper.

3 Calculations

In the following calculations we assume the parameters λ' and λ'' to be real. We will only consider the lowest order
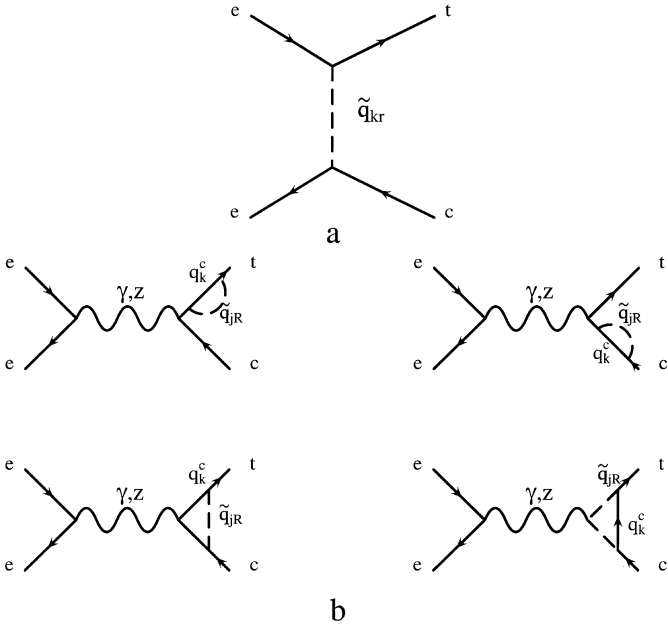
Fig. 1a,b. Feynman diagrams of $e^+e^- \rightarrow t\bar{c}$. **a** Tree-level diagrams from $L^{\lambda'}_{\not{R}_p}$. **b** One-loop diagrams from $L^{\lambda''}_{\not{R}_p}$, dashed lines represent sleptons and squarks
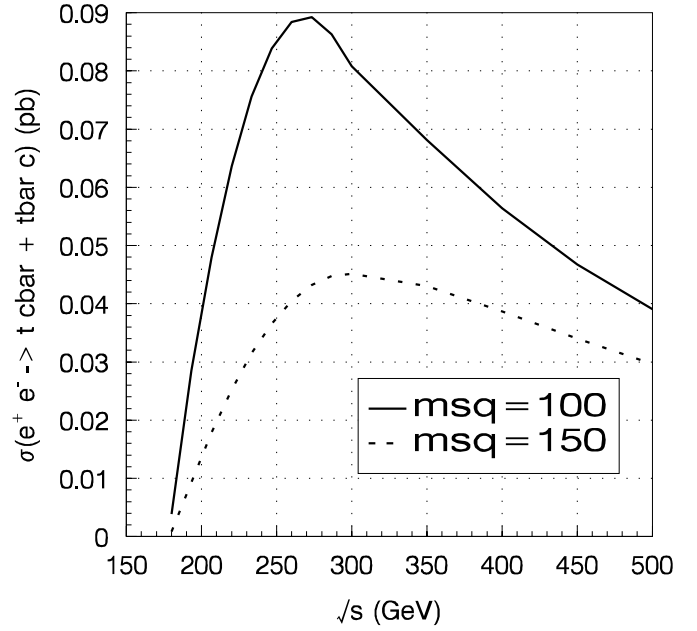

Fig. 2. Cross section of $e^+e^- \rightarrow t\bar{c} + c\bar{t}$ as a function of the c.m. energy $s^{1/2}$ with $\lambda'_{12j}\lambda'_{13j} = 0.01$. Solid line for $m_{\tilde{l}} = m_{\tilde{q}} = 100\,\text{GeV}$, and dashed line for $m_{\tilde{l}} = m_{\tilde{q}} = 150\,\text{GeV}$

effects from $L^{\lambda'}_{\not{R}_p}$ and $L^{\lambda''}_{\not{R}_p}$.

(A.) $e^+(p_3)e^-(p_4) \rightarrow t(p_1)\bar{c}(p_2)$ at tree level; recall the statement after (2.4).

We define the Mandelstam variables as usual:

$$s = (p_1 + p_2)^2 = (p_3 + p_4)^2, \qquad (3.a.1)$$

$$t = (p_1 - p_3)^2 = (p_4 - p_2)^2, \qquad (3.a.2)$$

$$u = (p_1 - p_4)^2 = (p_3 - p_2)^2. \qquad (3.a.3)$$

The amplitude (as shown in Fig. 1a) is given by

$$M = \Sigma_j \frac{i\lambda'_{13j}\lambda'_{12j}}{(t - m^2_{\text{squark}_j})}$$
$$\times \bar{u}(p_1)P_R u^c(p_3)\bar{v}^c(p_4)P_L v(p_2), \qquad (3.a.4)$$

where $P_{L,R}$ are left- and right-helicity projections, respectively, $j = 1, 2, 3$, and the upper index c means charge conjugate. The amplitude depends strongly on the products $\lambda'_{12j}\lambda'_{13j}$ ($j = 1, 2, 3$).

(B.) Contributions from $L^{\lambda''}_{\not{R}_p}$ terms (no contributions at tree level). If we set all λ' parameters to zero, we obtain the effects of $L^{\lambda''}_{\not{R}_p}$ terms within the present upper bounds. One-loop corrections (as shown in Fig. 1b) of $e^+(p_3)e^-(p_4) \rightarrow t(p_1)\bar{c}(p_2)$ are proportional to the products $\lambda''_{2ij}\lambda''_{3ij}$ ($i, j = 1, 2, 3$); thus it is possible to detect $\not{R}_p$-signals or get much stronger constraints on these parameters by measuring this process in future experiments.

Since the proper vertex counterterm should cancel with the counterterms of the external legs diagrams in this case, we do not have to deal with the ultraviolet divergence. Thus we simply take the sum of all (unrenormalized) reducible and irreducible diagrams and the result is finite and gauge invariant. In the Appendix we will give the details of the amplitudes.

(C.) Total cross sections. In a similar way we obtain the amplitude for the process $e^+e^- \rightarrow c\bar{t}$. Thus the total cross section for the process $e^+e^- \rightarrow t\bar{c} + c\bar{t}$ is

$$\hat{\sigma}(\hat{s}) = \frac{2N_c}{16\pi\hat{s}^2} \int_{\hat{t}^-}^{\hat{t}^+} d\hat{t} \overline{\sum}_{\text{spins}} [|M|^2], \qquad (3.5)$$

where M is the amplitude and $\hat{t}^{\pm} = (1/2)\left[(m_t^2 + m_c^2 - \hat{s}) \pm (\hat{s}^2 + m_t^4 + m_c^4 - 2\hat{s}m_t^2 - 2\hat{s}m_c^2 - 2m_t^2 m_c^2)^{1/2}\right]$. Here we have neglected the masses of the electron and the muon. $N_c = 3$ is the color factor and the bar over summation means averaging over initial spins.

Similarly we obtain the total cross section of $\mu^+\mu^- \rightarrow t\bar{c} + c\bar{t}$. Assuming values for all input parameters, we obtain our numerical results.

4 Numerical results

In the numerical calculations we assume $m_{\tilde{q}} = m_{\tilde{l}}$ and consider the effects from $L^{\lambda'}_{\not{R}_p}$ and $L^{\lambda''}_{\not{R}_p}$ separately. For the B-violating parameter $\lambda''_{2ij}\lambda''_{3ij}$ ($i, j = 1 - 3$), the upper bounds of λ''_{223} and λ''_{323} dominate all other parameters. Thus we neglect all other λ'' terms. For the L-violating parameters we set $\lambda'_{12j} = \lambda'_{13j} = 0.1$ ($j = 1, 2, 3$) when
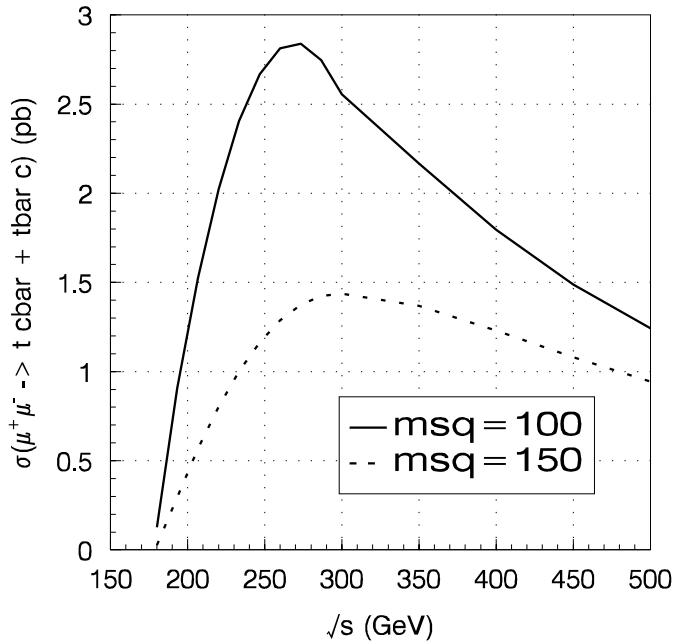
Fig. 3. Cross section of $\mu^+\mu^- \to t\bar{c} + c\bar{t}$ as a function of the c.m. energy $s^{1/2}$ with $\lambda'_{22j} = 0.18$ and $\lambda'_{23j} = 0.36$, see [5]
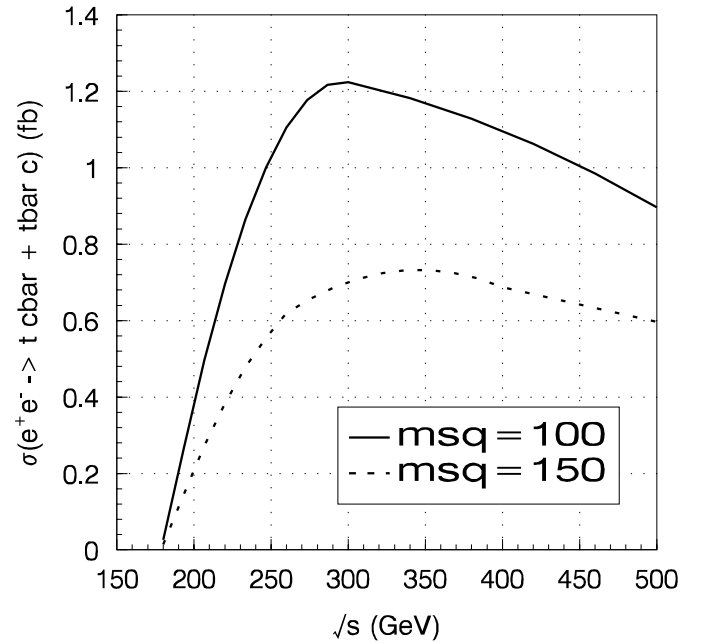
Fig. 4. Cross section of $e^+e^- \to t\bar{c} + c\bar{t}$ as a function of the c.m. energy $s^{1/2}$ with $\lambda''_{323}\lambda''_{223} = 0.625$. Solid line for $m_{\tilde{l}} = m_{\tilde{q}} = 100\,\mathrm{GeV}$, and dashed line for $m_{\tilde{l}} = m_{\tilde{q}} = 150\,\mathrm{GeV}$

$m_{\tilde{q}} = 100\,\mathrm{GeV}$, which agrees with the product coupling limits also. For the $\mu^+\mu^-$ colliders, the parameters λ'_{22j} and λ'_{23j} can be larger because they involve heavier flavor. In this case we use the data of [6].

In Fig. 2, we show the cross section of $e^+e^- \to t\bar{c} + c\bar{t}$ as a function of the c.m. energy of the electron–positron system at the upper bounds of λ', i.e. $\lambda'_{12j}\lambda'_{13j} = 0.01$. We take $m_{\tilde{l}} = m_{\tilde{q}} = 100\,\mathrm{GeV}$ (solid line) and $m_{\tilde{l}} = m_{\tilde{q}} = 150\,\mathrm{GeV}$ (dashed line), respectively. There we take same coupling parameters for different $m_{\tilde{q}}$ for comparing the effects of mass of squarks in the process. The results show that the cross sections can be 0.02 pb for the solid line and 0.006 pb for the dashed line at $s^{1/2} = 190\,\mathrm{GeV}$, which is the present LEP running energy. So if the electron–positron integrated luminosity is 150 pb^{-1} [7], we can expect about 3 events when $m_{\tilde{l}} = m_{\tilde{q}} = 100\,\mathrm{GeV}$. At $s^{1/2} = 200\,\mathrm{GeV}$ and luminosity about 200 pb^{-1}, we expect eight events from our results. Even if this sounds too optimistic, it may be worthwhile to consider this process once the LEP energy is above the threshold of single top-quark production. For the NLC, with c.m. energy about 500 GeV and luminosity about 50 fb^{-1}, thousands of events should be observed at the present upper bounds of the parameters.

In Fig. 3, we plot the cross section of $\mu^+\mu^- \to t\bar{c} + c\bar{t}$ as a function of the c.m. energy of the $\mu^+\mu^-$ system with the upper bounds of λ', i.e. $\lambda'_{22j} = 0.18$ and $\lambda'_{23j} = 0.36$ (see [6]). We take again $m_{\tilde{l}} = m_{\tilde{q}} = 100\,\mathrm{GeV}$ for the solid line and $m_{\tilde{l}} = m_{\tilde{q}} = 150\,\mathrm{GeV}$ for the dashed line. The cross sections are much larger than those of Fig. 2. That is because from the present data the upper limits of λ'_{22j} and λ'_{23j} are larger than those of λ'_{12j} and λ'_{13j}. The cross

section can be about 1 pb when $s^{1/2} = 200\,\mathrm{GeV}$, which means we can get hundreds of events at μ colliders with the same luminosity as LEP if the coupling parameters are close to the present upper limits.

In order to give more stringent constraints for λ'' in future experiments, we draw attention to the effects from possible B-violating terms in Fig. 4, where the cross section of $e^+e^- \to t\bar{c} + c\bar{t}$ as a function of the c.m. energy is given. (The solid line is for $m_{\tilde{l}} = m_{\tilde{q}} = 100\,\mathrm{GeV}$ and the dashed line for $m_{\tilde{l}} = m_{\tilde{q}} = 150\,\mathrm{GeV}$). When $\lambda''_{223}\lambda''_{323}$ is about 0.625 (see [6]), the cross section will be about 0.5 fb at $s^{1/2} = 200\,\mathrm{GeV}$ or 0.9 fb at $s^{1/2} = 500\,\mathrm{GeV}$. That corresponds to 0.1 event at LEP or 45 events at the NLC.

Let us compare the results with those from $\gamma\gamma \to t\bar{c} + c\bar{t}$ of [17]. It turns out that B-violating terms (i.e. $L^{\lambda''}_{\cancel{R}_p}$) give similar effects in both processes, whereas L-violation (i.e. $L^{\lambda'}_{\cancel{R}_p}$) contributes much less in $\gamma\gamma$ collisions than in e^+e^- processes. Therefore, a combination of the results of both these processes allows for a determination of the source for R_p-violation (i.e. either from L-violation or from B-violation)

5 Conclusion

We studied the processes $e^+e^- \to t\bar{c} + c\bar{t}$ and $\mu^+\mu^- \to t\bar{c} + c\bar{t}$ in a supersymmetric model with explicit R_p-violation. The calculations show that it is possible to test the model at future LEP and the future NLC experiments, provided the couplings (λ'-type) are large enough within the present experimentally admitted range. We can even detect possi-

ble B-violating terms in future lepton colliders with higher energy and higher luminosity than LEP. We also considered the possibility of production of $t\bar{c}$ and $c\bar{t}$ at $\mu^+\mu^-$ colliders. The results show that these colliders may allow one to test R_p-violation.

A Loop integrals

We adopt the definitions of two- and three- one-loop Passarino–Veltman integral functions in [18,19]. The integral functions are defined as follows.
(1) The two-point integrals are:

$$\{B_0; B_\mu; B_{\mu\nu}\}(p, m_1, m_2) = \frac{(2\pi\mu)^{4-n}}{\mathrm{i}\pi^2}$$
$$\times \int \mathrm{d}^n q \frac{\{1; q_\mu; q_\mu q_\nu\}}{[q^2 - m_1^2][(q+p)^2 - m_2^2]}. \quad (A.1)$$

The function B_μ should be proportional to p_μ:

$$B_\mu(p, m_1, m_2) = p_\mu B_1(p, m_1, m_2). \quad (A.2)$$

Similarly we get

$$B_{\mu\nu} = p_\mu p_\nu B_{21} + g_{\mu\nu} B_{22}. \quad (A.3)$$

We denote $\bar{B}_0 = B_0 - \Delta$, $\bar{B}_1 = B_1 + (1/2)\Delta$ and $\bar{B}_{21} = B_{21} - (1/3)\Delta$. with $\Delta = (2/\epsilon) - \gamma + \log(4\pi)$, $\epsilon = 4 - n$. μ is the scale parameter.
(2) The three-point integrals are

$$\{C_0; C_\mu; C_{\mu\nu}; C_{\mu\nu\rho}\}(p, k, m_1, m_2, m_3) = -\frac{(2\pi\mu)^{4-n}}{\mathrm{i}\pi^2} \times$$
$$\int \mathrm{d}^n q \frac{\{1; q_\mu; q_\mu q_\nu; q_\mu q_\nu q_\rho\}}{[q^2 - m_1^2][(q+p)^2 - m_2^2][(q+p+k)^2 - m_3^2]}. \quad (A.4)$$

We can express the tensor integrals through scalar functions in the following way:

$$C_\mu = p_\mu C_{11} + k_\mu C_{12},$$

$$C_{\mu\nu} = p_\mu p_\nu C_{21} + k_\mu k_\nu C_{22} + (p_\mu k_\nu + k_\mu p_\nu) C_{23} + g_{\mu\nu} C_{24}$$

$$C_{\mu\nu\rho} = p_\mu p_\nu p_\rho C_{31} + k_\mu k_\nu k_\rho C_{32} + (k_\mu p_\nu p_\rho + p_\mu k_\nu p_\rho + p_\mu p_\nu k_\rho) C_{33} + (k_\mu k_\nu p_\rho + p_\mu k_\nu k_\rho + k_\mu p_\nu k_\rho) C_{34} + (p_\mu g_{\nu\rho} + p_\nu g_{\mu\rho} + p_\rho g_{\mu\nu}) C_{35} + (k_\mu g_{\nu\rho} + k_\nu g_{\mu\rho} + k_\rho g_{\mu\nu}) C_{36}. \quad (A.5)$$

The numerical calculation of the vector and tensor loop integral functions can be traced back to the four scalar loop integrals A_0, B_0 and C_0 in [12,13] and the references therein.

B One-loop correction of the amplitude

The amplitude of one-loop diagrams δM from $L_{\hat{R}_p}^{\lambda''}$ (Fig. 1b) can be decomposed into δM_γ and δM_Z terms with

$$\delta M_\gamma = \frac{e g_{\mu\nu}}{s} \bar{v}(p_3)\gamma^\nu$$
$$\times u(p_4)\bar{u}(p_1)\Sigma_\gamma^\nu(p_1, p_2)v(p_2), \quad (B.1)$$

and

$$\delta M_Z = \left(\frac{e}{4c_{\mathrm{w}}s_{\mathrm{w}}}\right) \frac{g_{\mu\nu} - k_\mu k_\nu/m_z^2}{s - m_Z^2}$$
$$\times \bar{v}(p_3)\gamma^\nu((2 - 4s_{\mathrm{w}}^2)P_{\mathrm{L}} - 4s_{\mathrm{w}}^2 P_{\mathrm{R}})$$
$$\times u(p_4)\bar{u}(p_1)\Sigma_Z^\nu(p_1, p_2)v(p_2), \quad (B.2)$$

where $k = p_1 + p_2$, $e^2/4\pi = \alpha = 1/137.04$, $c_{\mathrm{w}} = \cos\theta_{\mathrm{W}}$, $s_{\mathrm{w}} = \sin\theta_{\mathrm{W}}$ and θ_{W} is the Weinberg-angle and $\Sigma_{\gamma,Z}^\nu(p_1, p_2)$ is defined as follows:

$$\Sigma_{\gamma,Z}^\nu(p_1, p_2) = V_{\gamma,Z}^{(1)}P_{\mathrm{R}}\gamma^\nu + V_{\gamma,Z}^{(2)}P_{\mathrm{R}}p_1^\nu + V_{\gamma,Z}^{(3)}P_{\mathrm{R}}p_2^\nu$$
$$+ V_{\gamma,Z}^{(4)}P_{\mathrm{L}}\gamma^\nu + V_{\gamma,Z}^{(5)}P_{\mathrm{L}}p_1^\nu + V_{\gamma,Z}^{(6)}P_{\mathrm{L}}p_2^\nu. \quad (B.3)$$

Here the $V_{\gamma,Z}^{(i)}$ are scalar functions of p_1, p_2.

References

1. H.E. Haber, G.L. Kane, Phys. Rep. **117**, 75 (1985); J.F. Gunion, H.E. Haber, Nucl. Phys. B **272**, 1 (1986)
2. G. Farrar, P. Fayet, Phys. Lett. B **76**, 575 (1978)
3. L.J. Hall, M. Suzuki, Nucl. Phys. B **231**, 419 (1984)
4. Y. Fukuda et al, Phys. Rev. Lett., **81**, 1562 (1998)
5. C. Adloff et al, Z. Phys. C **74**, 191 (1997); J. Breitweg et al, Z. Phys. C **74**, 207 (1997); J. Butterworth, H. Dreiner, Nucl. Phys. B **397**, 3 (1993)
6. S. Weinberg, Phys. Rev. D **26**, 287 (1982); P. Roy, TIFR/TH/97-60; D.K. Ghosh, S. Raychaudhburi, K. Sridbar, Phys. Lett. B **396**, 177 (1997); K. Agashe, M. Graesser, Phys. Rev. D **54**, 4445 (1996); K. Huitu, J. Maalampi, M. Raidl, A. Santamaria, Phys. Lett. B **430**, 355 (1998); J-H. Jiang, J.G. Kim, J.S. Lee, Phys. Rev. D **55**, 7296 (1997); Phys. Lett. B **408**, 367 (1997); Phys. Rev. D **58**, 035006 (1998); G. Bhattacharyya, D. Choudhury, K. Sridhar, Phys. Lett. B **355**, 193 (1995); J. Ferrandis, Phys. Rev. D **60**, 095012 (1999); M.A. Diaz, J. Ferrandis, J.C. Romao, J.W. F. Valle, Phys. Lett. B 453; M.A. Diaz, J. Ferrandis, J.C. Romao, J.W.F. Valle, hep-ph/9906343; M.A. Diaz, J. Ferrandis, J.W.F. Valle, hep-ph/9909212; B.C. Allanach, A. Dedes, H.K. Dreiner, Phys. Rev. D **60**, 075014 (1999)
7. R. Barbier et al, hep-ph/9810232; B. Allanach et al, hep-ph/9906224
8. U. Mahanta, A. Ghosal, Phys. Rev. D **57**, 1735 (1998); M. Chemtob, G. Moreau, Phys. Rev. D **59**, 116012 (1999)
9. C.D. Froggatt, H.B. Nielsen, Nucl. Phys. B **147**, 277 (1979)

10. D. Choudhury, Phys. Lett. B **376**, 201 (1996); D.K. Ghosh et al. in [6]; J. Kalinowski, R. Rueckl, H. Spiesberger, P.M. Zerwas, Phys. Lett. B **414**, 297 (1997); D. Choudhury, S. Raychaudhuri, hep-ph/9807373

11. C.S. Huang et al. Phys. Lett. B **452**, 143 (1999)

12. D. Atwood et al. Phys. Rev. D **53**, 1199 (1996); D. Atwood, L. Reina, A. Soni, Phys. Rev. Lett.**75**, 3800 (1995); W-S. Hou, G-L. Lin, Phys. Lett. B **379**, 261 (1996); Y. Jiang, M-l. Zhou, W-G. Ma, L. Han, H. Zhou, M. Han, Phys. Rev. D **57**, 4343 (1998)

13. S. Dimopoulos, G.F. Giudice, N. Tetradis, Nucl. Phys. B **454**, 59 (1995)

14. R. Hempfling, Nucl. Phys. B **478**, 3 (1996); B. Mukhopadhay, S. Roy, Phys. Rev. D **55**, 7020 (1997)

15. S. Dimopoulos, L.J. Hall, Phys. Lett. B **207**, 210 (1987); V. Barger,G.F. Giudice, T. Han, Phys. Rev. D **40**, 2987 (1989)

16. S. Bar-Shalom, G. Eilam, A. Soni, Phys. Rev. D **60**, 035007 (1999)

17. Z-H.Yu, H. Pietschmann, W-G.Ma, L. Han, Y. Jiang, hep-ph/9903471

18. Bernd A. Kniehl, Phys. Rep. **240**, 211 (1994)

19. G. Passarino, M. Veltman, Nucl. Phys. B **160**, 151 (1979)